Supporting Information for:

Solvent-Engineered Design of Argyrodite Li_6PS_5X (X= Cl, Br, I) Solid Electrolytes with High Ionic Conductivity

Laidong Zhou, [a] *Kern-Ho Park,* [a] *Xiaoqi Sun,* [a] *Fabien Lalère,* [a] *Torben Adermann,* [b] *Pascal Hartmann,* [b] *and Linda F. Nazar* [a*]

[a] Department of Chemistry and the Waterloo Institute for Nanotechnology, University of Waterloo, 200 University Ave W, Waterloo, Ontario N2L 3G1, Canada

[b] BASF SE, Ludwigshafen 67063, Germany

Experimental methods

Material synthesis and characterization. In an argon-filled glovebox, a stoichiometric 3:1 molar ratio of Li_2S (Sigma-Aldrich, 99.98%) and P_2S_5 (Sigma-Aldrich, 99%) were mixed in an agate mortar and dispersed in anhydrous tetrahydrofuran (THF).[1] The mixture was stirred for 24 h at room temperature to obtain a β-Li_3PS_4·3THF/THF suspension. Li_2S (Sigma-Aldrich, 99.98%) and LiX (Sigma-Aldrich, >99%) with the targeted molar ratio were dissolved in anhydrous ethanol, and the solution was added to the above suspension. The color of the mixture changed immediately after addition and the white precipitates gradually dissolved. After stirring overnight, the mixture was centrifuged at 8000 rpm for 10 min to remove any unreacted precipitates. The obtained clear solution was dried under vacuum to remove the solvents. The obtained pale yellow powder was further dried in a Buchi oven at 140°C for 20 h under vacuum to remove remaining solvents. Finally, the poorly crystallized powder was pressed into a pellet and sealed in a carbon-coated quartz tube under vacuum, then annealed at 550°C for 6h with a ramp rate of 5°C/min to obtain the fully crystallized Li_6PS_5X or $Li_{6-y}PS_{5-y}Cl_{1+y}$ (y = 0 - 0.5) products.

Li_3PS_4·3THF powder could also be directly used as the precursor (from BASF SE, Germany). In this case, Li_2S (Sigma-Aldrich, 99.98%) and LiX (Sigma-Aldrich, >99%) in the targeted molar ratio were dissolved in anhydrous ethanol, and the required amount of Li_3PS_4·3THF powder was added to the solution. The white Li_3PS_4·3THF powder dissolved gradually and a clear solution was obtained after 30 min. The solution was stirred overnight and died under vacuum. The obtained pale yellow powder was further dried and crystallized following above-mentioned procedures.

Solid state synthesized Li_6PS_5Cl was prepared by mechanical ball milling of a stoichiometric mixture of Li_2S (Sigma-Aldrich, 99.98%) and P_2S_5 (Sigma-Aldrich, 99%) and LiCl (Sigma-Aldrich, >99%) in ZrO_2 jars with ZrO_2 balls and milled at 400RPM for 15h using a high energy planetary ball mill (Fritsch PULVERISETTE 7 Premium). The milled powder was pressed into pellets, sealed in a carbon-coated quartz tube under vacuum and sintered at 550°C for 6h with a ramp rate of 5°C/min to crystallize the material.

Material morphologies were examined using a Zeiss field emission scanning electron microscope (SEM) equipped with an energy dispersive X-ray spectroscopy detector (EDX). The samples were transferred to the SEM for imaging with a second exposure to air, via a specially designed transfer holder.

Powder diffraction and refinement. X-ray diffraction (XRD) measurements were conducted at room temperature on a PANalytical Empyrean diffractometer with Cu-Kα radiation equipped with a PIXcel bidimensional detector. XRD patterns for phase identification were obtained in Bragg-Brentano geometry, with samples placed on a zero-background sample holder in an Ar-filled glovebox and protected by Kapton film. Standard addition analysis (degree of crystallinity measurements) was carried out by mixing the sample with 10 wt% Si (standard silicon, 325 mesh, Sigma-Aldrich, 99%), which was used as external reference in Rietveld Refinements, in an Ar-filled glovebox and the mixture was sealed in 0.3 mm glass capillaries. XRD patterns were collected in Debye-Scherrer geometry. Rietveld refinement[2] was performed using the FullProf suite. [3] Scale factor, zero point, background, lattice parameters, phase fraction, fraction coordinates, occupancies, and thermal parameters were sequentially refined for all phases, allowing determination of the fraction of the major argyodite and the impurities.

Conductivity measurements. Ionic conductivities were measured by electrochemical impedance spectroscopy (EIS). Typically, 100 mg of the Li_6PS_5X and $Li_{6-y}PS_{5-y}Cl_{1+y}$ powder was placed between two stainless steel rods and pressed into a 10 mm diameter pellet by a hydraulic press at two tons for 3 min in an argon-filled glovebox. The thickness of the pellet was close to 0.6 - 0.8mm depending on the materials (accurately measured by a caliper for each pellet), and the relative density of the pellets was around 99%; this vale was calculated from the sample geometry and mass and compared to the theoretical density of Li_6PS_5Cl (1.64 g•cm^{-3}) and Li_6PS_5Br (1.90 g•cm^{-3}). EIS was performed with a 20 mV constant voltage within a frequency range of 1 MHz-10 mHz using a VMP3 potentiostat/galvanostat (Bio-logic). Error was estimated by the inaccuracy in measuring the pellet thickness, determined over multiple measurements. Direct-current (DC) polarization measurements were conducted on the pellets with applied voltages of 0.25 V, 0.5 V and 0.75 V for 30 min each to determine the electronic conductivity of the argryodites.

Galvanostatic cycling studies. For the galvanostatic cycling study of the solid state cells, working electrodes were prepared by mixing TiS_2 and Li_6PS_5Cl powder in a weight ratio of 1:1. $Li_{11}Sn_6$ alloy was prepared by mixing Li foil (Sigma-Aldrich, 99.9%) and Sn powder (Fisher scientific), and used as counter electrode. $Li_{11}Sn_6$ alloy lies at a potential of 0.49 V (vs. Li/Li$^+$, see below, **Fig. S8**), which is in accord with a previous report.[4] The solid electrolyte layer was formed by pressing 100 mg of Li_6PS_5Cl powder. The as-prepared electrode mixture (6 mg) and $Li_{11}Sn_6$ (30 mg) were spread on both sides of a Li_6PS_5Cl pellet, followed by pressing at 374 MPa. All the assembly was carried out in a poly(aryl-ether-ether-ketone (PEEK) mold (diameter: 10 mm) with two Ti rods as the current collectors. The galvanostatic charge-discharge studies were conducted with a current density of 100 μA cm^{-2} (0.11 C).

List of Supporting Figures

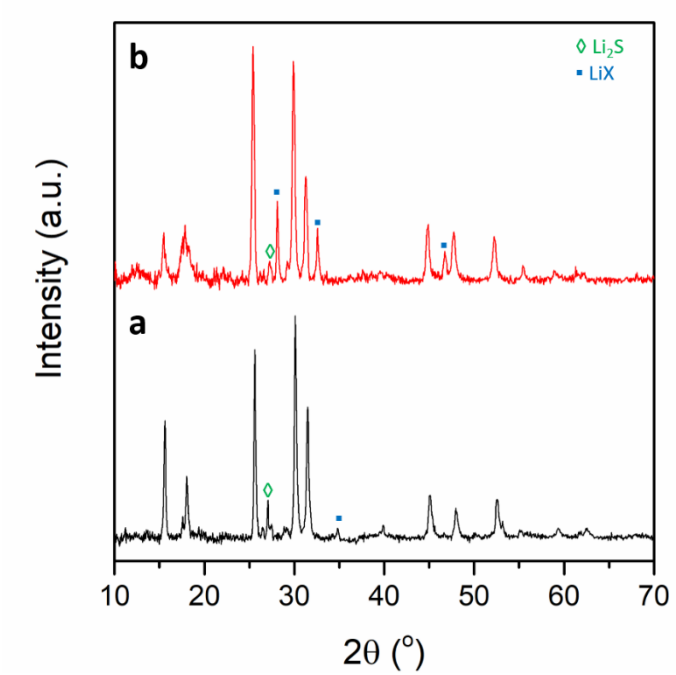

Figure S1: XRD patterns of: (a) Li_6PS_5Cl and (b) Li_6PS_5Br from solution synthesis after drying at 140°C for 20 h under vacuum (all reflections correspond to the respective argyrodite phase except for the impurities as marked).

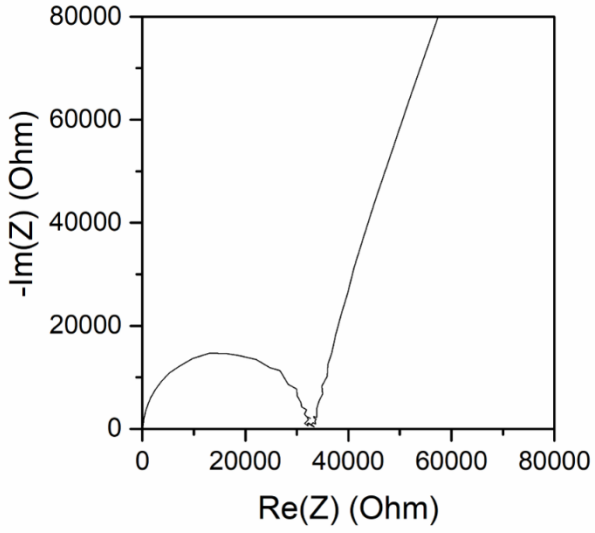

Figure S2: Nyquist plot for the Li_6PS_5I solid electrolyte (cold-pressed at 2 tons, measured at 300K, in the frequency range from 1 MHz-10 mHz).

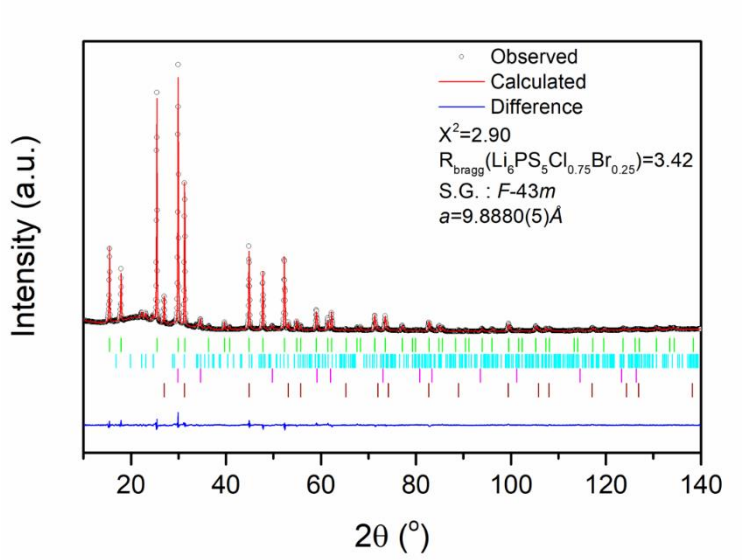

Figure S3: Rietveld refinement of XRD patterns of $Li_6PS_5Cl_{0.75}Br_{0.25}$. Black circles – experimental data; red lines – fitted data; blue lines – difference curve between observed and calculated data; ticks – the Bragg peak positions of Li_6PS_5 $Cl_{0.75}Br_{0.25}$ (green), Li_3PO_4 (cyan), $LiCl_{0.75}Br_{0.25}$ (magenta) and Li_2S (burgundy).

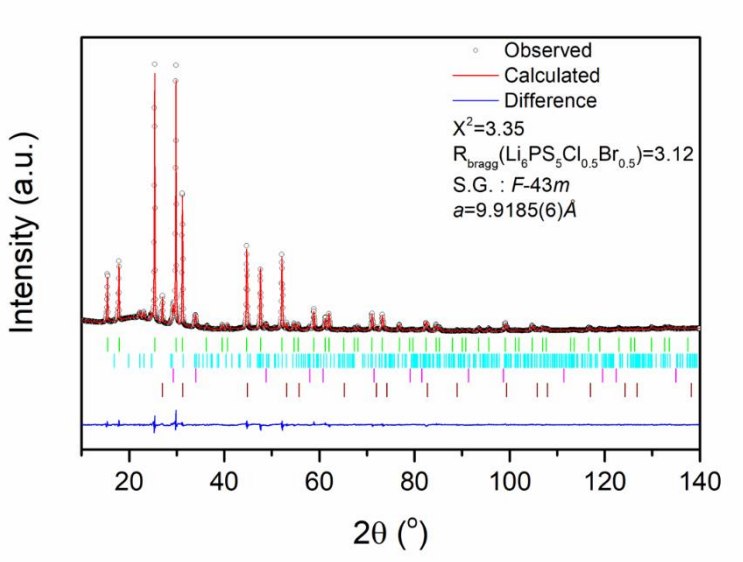

Figure S4: Rietveld refinement of XRD patterns of $Li_6PS_5Cl_{0.5}Br_{0.5}$. Black circles – experimental data; red lines – fitted data; blue lines – difference curve between observed and calculated data; ticks – the Bragg peak positions of Li_6PS_5 $Cl_{0.5}Br_{0.5}$ (green), Li_3PO_4 (cyan), $LiCl_{0.5}Br_{0.5}$ (magenta) and Li_2S (burgundy).

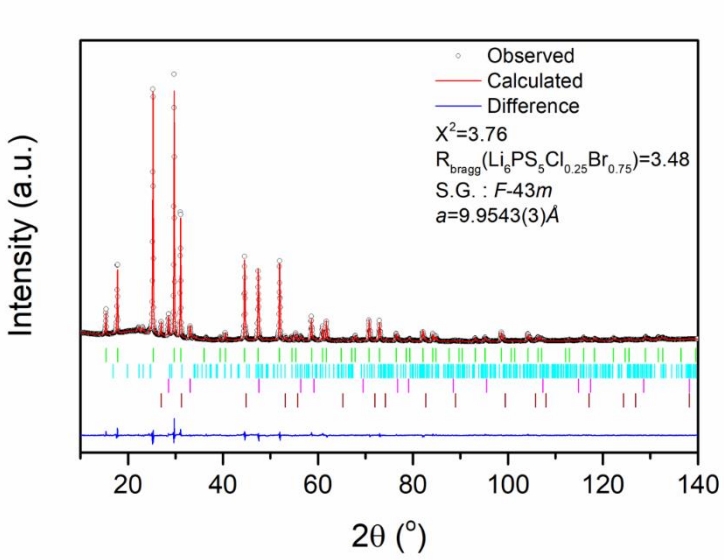

Figure S5: Rietveld refinement of XRD patterns of $Li_6PS_5Cl_{0.25}Br_{0.75}$. Black circles – experimental data; red lines – fitted data; blue lines – difference curve between observed and calculated data; ticks – the Bragg peak positions of Li_6PS_5 $Cl_{0.25}Br_{0.75}$ (green), Li_3PO_4 (cyan), $LiCl_{0.25}Br_{0.75}$ (magenta) and Li_2S (burgundy).

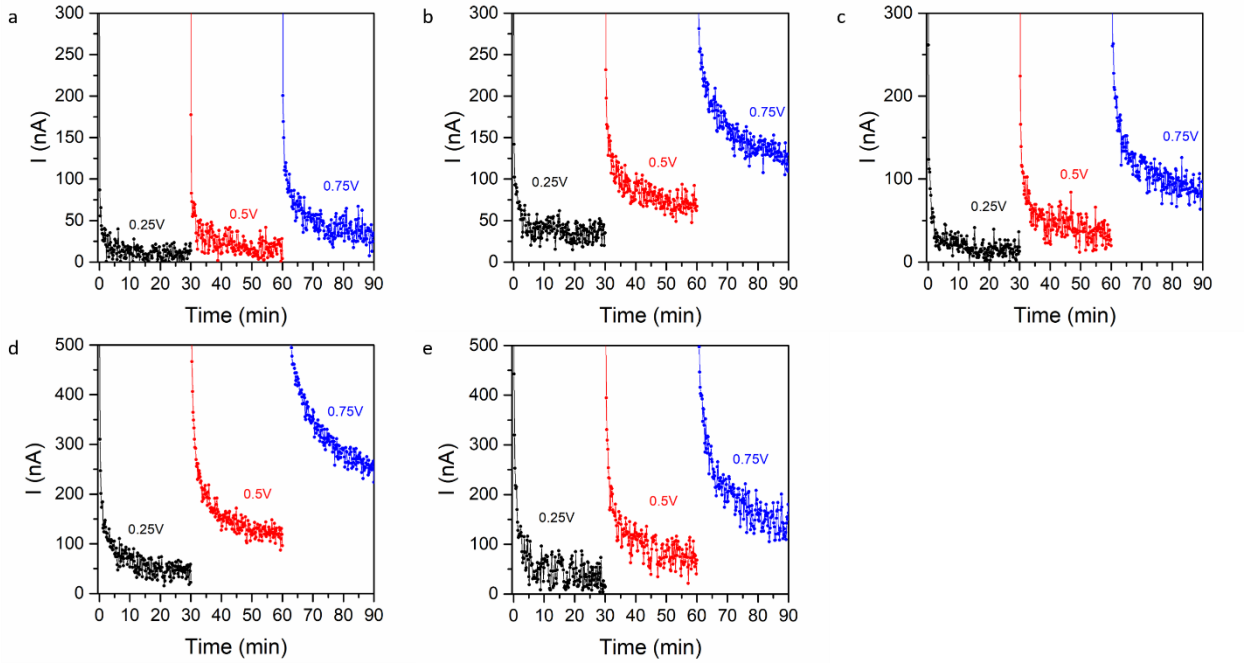

Figure S6: DC polarization curves of (a) $Li_6PS_5Cl_{0.75}Br_{0.25}$, (b) $Li_6PS_5Cl_{0.5}Br_{0.5}$, (c) $Li_6PS_5Cl_{0.75}Br_{0.25}$, (d) $Li_{5.75}PS_{4.75}Cl_{1.25}$ and (e) $Li_{5.5}PS_{4.5}Cl_{1.5}$ solid electrolytes with applied voltages of 0.25 V (black), 0.5 V (red), 0.75 V (blue) (cold-pressed at two tons, measured at 300K).

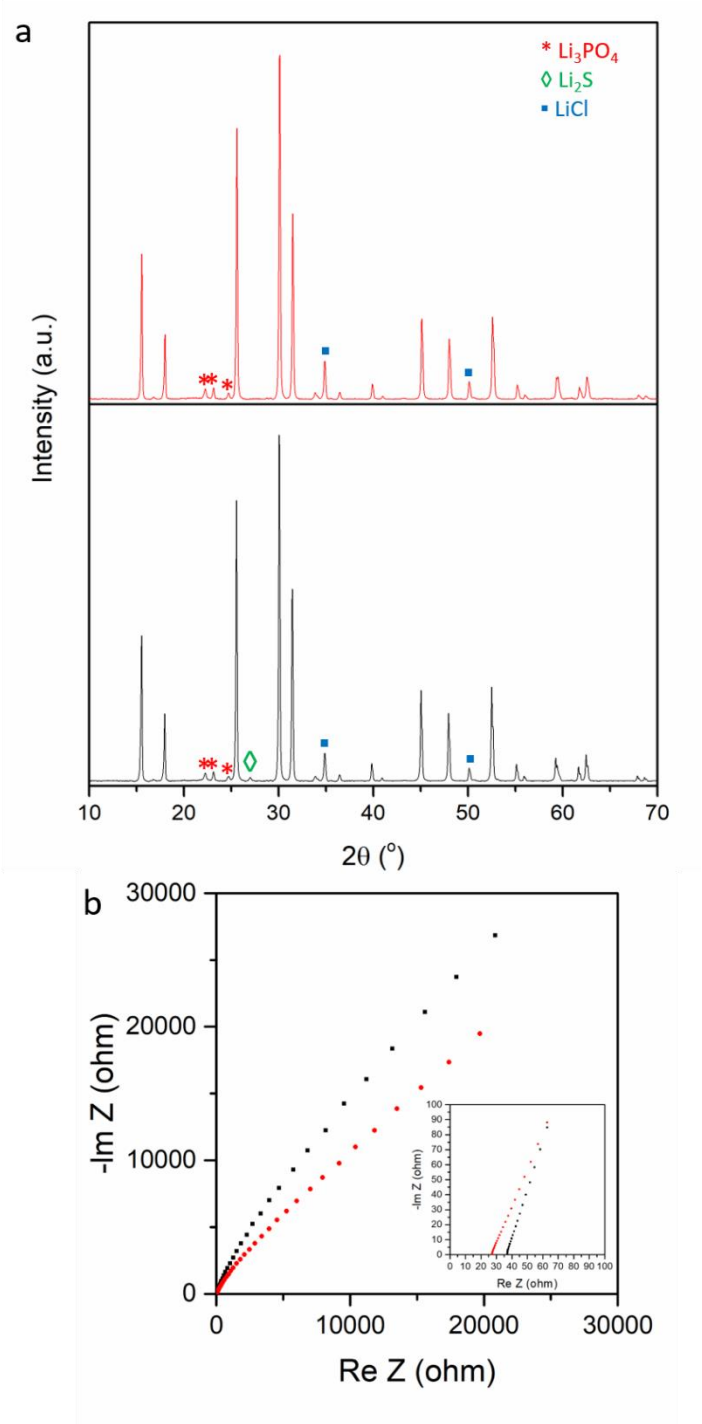

Figure S7: (a) XRD patterns of $Li_{5.75}PS_{4.75}Cl_{1.25}$ (black) and $Li_{5.5}PS_{4.5}Cl_{1.5}$ (red) from solution synthesis (all reflections correspond to the respective argyrodite phase except for the impurities as marked); (b) Nyquist plots for $Li_{5.75}PS_{4.75}Cl_{1.25}$ (black squares) and $Li_{5.5}PS_{4.5}Cl_{1.5}$ (red dots) (cold-pressed at 2 tons, measured at 300K, in the frequency range from 1 MHz-10 mHz).

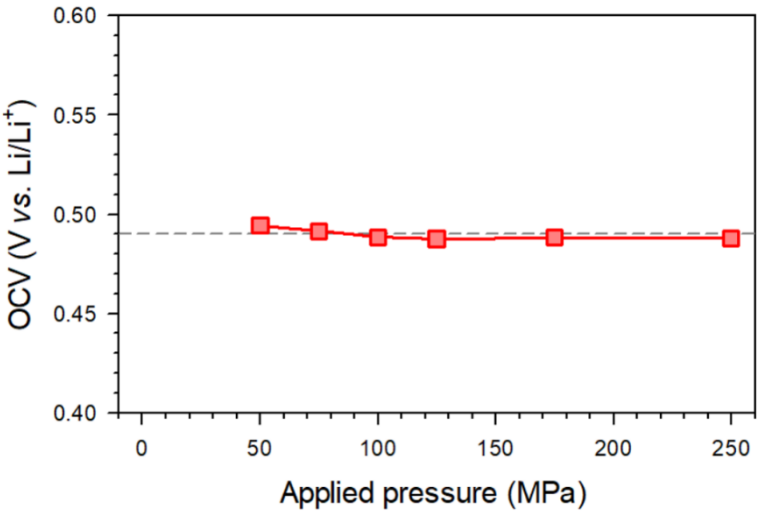

Figure S8: The open circuit voltage of the $Li_{11}Sn_6$/Li cell under applied cell pressure.

List of Supporting Tables

Table S1. Refined parameters for Li_6PS_5Cl (space group = *F*-43*m*, a = 9.8598(3) Å, R_{Bragg} = 4.83, X^2=4.50).

Atom	Wyckoff Site	*x*	*y*	*z*	Occ.	B_{iso} (Å^2)
Li1	48*h*	0.3205	0.0182	0.6798	0.5	2
Cl1	4*a*	0	0	0	0.385	2.5(2)
Cl2	4*d*	0.75	0.75	0.75	0.615	2.5(2)
P1	4*b*	0	0	0.5	1	1.7(1)
S1	16*e*	0.1195(2)	-0.1195(2)	0.6195(2)	1	2.99(5)
S2	4*a*	0	0	0	0.615	2.5(2)
S3	4*d*	0.75	0.75	0.75	0.385	2.5(2)

Table S2. Refined parameters for Li_6PS_5Br (space group = *F*-43*m*, a = 9.9855(4) Å, R_{Bragg} = 3.26, X^2 = 4.71).

Atom	Wyckoff Site	*x*	*y*	*z*	Occ.	B_{iso} (Å^2)
Li1	48*h*	0.3071	0.0251	0.6929	0.441	2
Li2	24*g*	0.25	0.017	0.75	0.119	2
Br1	4*a*	0	0	0	0.785(2)	2.9(1)
Br2	4*d*	0.75	0.75	0.75	0.215(2)	1.6(1)
P1	4*b*	0	0	0.5	1	1.3(1)
S1	16*e*	0.1184(2)	-0.1184(2)	0.6184(2)	1	1.97(7)
S2	4*a*	0	0	0	0.215(2)	2.9(1)
S3	4*d*	0.75	0.75	0.75	0.785(2)	1.6(1)

Table S3. Refined parameters for $Li_6PS_5Cl_{0.75}Br_{0.25}$ (space group = *F*-43*m*, a = 9.8880(4) Å, R_{Bragg} = 3.42, X^2=2.90).

Atom	Wyckoff Site	*x*	*y*	*z*	Occ.	B_{iso} (Å^2)
Li1	48*h*	0.3166	0.0178	0.6834	0.5	2
Br1	4*a*	0	0	0	0.22(2)	2.9(2)
Cl1	4*a*	0	0	0	0.26(2)	2.9(2)
Br2	4*d*	0.75	0.75	0.75	0.04(2)	1.3(2)
Cl2	4*d*	0.75	0.75	0.75	0.49 (2)	1.3(2)
P1	4*b*	0	0	0.5	1	1.54(8)
S1	16*e*	0.1200(2)	-0.1200(2)	0.6200(2)	1	2.99(5)
S2	4*a*	0	0	0	0.53(2)	2.9(2)
S3	4*d*	0.75	0.75	0.75	0.47(2)	1.3(2)

Table S4. Refined parameters for $Li_6PS_5Cl_{0.5}Br_{0.5}$ (space group = *F*-43*m*, a = 9.9185(6) Å, R_{Bragg} = 3.12, X^2=3.35).

Atom	Wyckoff Site	*x*	*y*	*z*	Occ.	B_{iso} (Å^2)
Li1	48*h*	0.3132	0.0212	0.6868	0.5	2
Br1	4*a*	0	0	0	0.39(2)	3.0(2)
Cl1	4*a*	0	0	0	0.20(2)	3.0(2)
Br2	4*d*	0.75	0.75	0.75	0.11(2)	1.4(2)
Cl2	4*d*	0.75	0.75	0.75	0.30(2)	1.4(2)
P1	4*b*	0	0	0.5	1	1.6(1)
S1	16*e*	0.1194(2)	-0.1194(2)	0.6194(2)	1	2.86(6)
S2	4*a*	0	0	0	0.41(2)	3.0(2)
S3	4*d*	0.75	0.75	0.75	0.59(2)	1.4(2)

Table S5. Refined parameters for $Li_6PS_5Cl_{0.25}Br_{0.75}$ (space group = *F*-43*m*, a = 9.9543(3) Å, R_{Bragg} = 3.48, X^2=3.76).

Atom	Wyckoff Site	*x*	*y*	*z*	Occ.	B_{iso} (Å^2)
Li1	48*h*	0.3138	0.0235	0.6862	0.5	2
Br1	4*a*	0	0	0	0.61(2)	2.79(9)
Cl1	4*a*	0	0	0	0.10(2)	2.79(9)
Br2	4*d*	0.75	0.75	0.75	0.14(2)	1.4(1)
Cl2	4*d*	0.75	0.75	0.75	0.15(2)	1.4(1)
P1	4*b*	0	0	0.5	1	1.02(7)
S1	16*e*	0.1191(1)	-0.1191(1)	0.6191(1)	1	2.05(4)
S2	4*a*	0	0	0	0.29(2)	2.79(9)
S3	4*d*	0.75	0.75	0.75	0.71(2)	1.4(1)

REFERENCES

(1) Liu, Z.; Fu, W.; Payzant, E. A.; Yu, X.; Wu, Z.; Dudney, N. J.; Kiggans, J.; Hong, K.; Rondinone, A. J.; Liang, C. Anomalous High Ionic Conductivity of Nanoporous β-Li_3PS_4. *J. Am. Chem. Soc.* **2013**, *135*, 975-978.

(2) Rietveld, H. M. A Profile Refinement Method for Nuclear and Magnetic Structures. *J. Appl. Cryst.* **1969**, *2*, 65-71.

(3) Rodríguez-Carvajal, J. Recent Advances in Magnetic Structure Determination by Neutron Powder Diffraction. *Physica. B: Condensed Matter.* **1993**, *192*, 55-69.

(4) Mayo, M.; Morris, A. J. Structure Prediction of Li-Sn and Li-Sb Intermetallics for Lithium-ion Batteries Anodes. *Chem. Mater.* **2017**, *29*, 5787-5795.